Competing Magnetic Exchange Interactions in Tetranuclear d^1 Systems: Synthesis, Structure, and Magnetochemistry of a Neutral Vanadium(IV) Complex with a $\{(VO)_4(\mu_3\text{-}OR)_2(\mu_2\text{-}OR)_4\}^{2+}$ Core

Winfried Plass*

Fakultät für Chemie, Lehrstuhl für Anorganische Chemie I, Universität Bielefeld, Postfach 100131, D-33501 Bielefeld, Germany

Received November 14, 1996[⊗]

The complex $[\{VO(L)\}_2\{VO(acac)\}_2(\mu_2\text{-}OMe)_2]$ **1** can be synthesized by reaction of the Schiff base ligand *N*,*N*-bis(2-hydroxyethyl)-*N*′-(2-pyrrolylmethylidene)ethylenediamine (H_2L) with $[VO(acac)_2]$ (Hacac = 2,4-pentanedione). The compound **1**·MeOH has been characterized by IR, UV/vis, and ESR spectroscopy as well as magnetic susceptibility measurements. A single-crystal diffraction study performed on **1**· MeOH gives the following crystal data: triclinic, $P\bar{1}$, $a = 7.352(2)$ Å, $b = 12.584(4)$ Å, $c = 12.826(4)$ Å, $\alpha = 107.61(2)°$, $\beta = 102.96(2)°$, $\gamma = 95.25(2)°$, $Z = 1$. The tetranuclear $\{(VO)_4(\mu_3\text{-}OR)_2(\mu_2\text{-}OR)_4\}^{2+}$ core of **1** is composed of three different types of edge-shared binuclear units, an *anti*-coplanar, two *syn*-coplanar, and two twist configurations. Consistent with this connectivity pattern, analysis of the magnetic data reveals competing ferromagnetic and antiferromagnetic exchange interactions within the tetranuclear core structure. Both ESR and magnetic data indicate a singlet ground state for **1**. In addition, the general magnetic behavior of oxovanadium(IV) clusters is discussed on the basis of classification schemes derived from simple binuclear fragmentation patterns. Consistent with the superexchange mechanism expected to be operative for binuclear oxovanadium(IV) units with *syn*-coplanar configuration, the corresponding magnetic exchange parameter J_{sc} of **1** ($V\cdots V = 3.410(2)$ Å) is determined to be antiferromagnetic at -153 cm^{-1}.

Introduction

Polynuclear transition-metal systems and especially their magnetic properties have become a subject of considerable interest in the last few years.[1] This is mainly based on their relevance for the understanding of the function of metalloproteins as well as their potential applications as magnetic materials.[2] Although interesting magnetic properties have been discovered for several systems, the detailed analysis of the magnetochemistry of such polynuclear transition-metal systems continues to be a field of growing interest.[3] In particular, well-characterized oxovanadium(IV) clusters for which the magnetic properties have been analyzed are still rather rare.[4−6] Here, the recently given classification for binuclear systems with a $\{VO(\mu_2\text{-}OR)_2VO\}^{2+}$ core can provide a valuable tool, as it shows a correlation with the observed magnetic properties.[7] This magnetostructural relationship is particularly appealing since edge-shared binuclear units are one of the basic structural motifs found in polynuclear oxovanadium(IV) clusters.

Given the clear coordination requirements set up by the vanadyl group, the reported magnetostructural relationship[7] can be generally applied to edge-shared binuclear units independent of the actual coordination mode at the individual oxovanadium(IV) centers, i.e., octahedral or square pyramidal. Therefore, only the relative orientation of the vanadyl groups within a binuclear unit is necessary in order to qualitatively predict its magnetic behavior in terms of antiferro- (*syn*- and *anti*-orthogonal and *syn*-coplanar) or ferromagnetic interactions (*anti*-coplanar and twist) between the metal centers. Although a different notation is necessary, this concept can basically be extended to oxovanadium(IV) centers in a vertex-shared bridging mode, which is yet another fundamental structural motif in the construction of polynuclear oxovanadium(IV) clusters.[8] The

* E-mail: winfried.plass@post.uni-bielefeld.de.

⊗ Abstract published in *Advance ACS Abstracts,* April 15, 1997.

(1) Recent examples (see also references cited therein): (a) Sessoli, R.; Gatteschi, D.; Caneschi, A.; Novak, M. A. *Nature* **1993**, *365*, 141. (b) Eppley, H. J.; Tsai, H.-L.; de Vries, N.; Folting, K.; Christou, G.; Hendrickson, D. N. *J. Am. Chem. Soc.* **1995**, *117*, 301. (c) Powell, A. K.; Heath, S. L.; Gatteschi, D.; Pardi, L.; Sessoli, R.; Spina, G.; Del Giallo, F.; Pieralli, F. *J. Am. Chem. Soc.* **1995**, *117*, 2491. (d) Goldberg, D. P.; Caneschi, A.; Delfs, C. D.; Sessoli, R.; Lippard, S. J. *J. Am. Chem. Soc.* **1995**, *117*, 5789. (e) Benelli, C.; Parsons, S.; Solan, G. A.; Winpenny, R. E. P. *Angew. Chem., Int. Ed. Engl.* **1996**, *35*, 1825.

(2) (a) *Magneto-Structural Correlations in Exchange Coupled Systems*; Willet, R. D., Gatteschi, D., Kahn, O., Eds.; Riedel: Dordrecht, The Netherlands, 1985. (b) *Magnetic Molecular Materials*; Gatteschi, D., Kahn, O., Miller, J. S., Palacio, F., Eds.; Kluwer: Dodrecht, The Netherlands, 1991; pp 157−169. (c) Kahn, O. *Molecular Magnetism*; VCH Publishers: New York, 1993. (d) *Biomimetic Materials Chemistry*; Mann, S., Ed.; VCH Publishers: New York, 1995.

(3) Recent examples (see also references cited therein): (a) Caneschi, A.; Gatteschi, D.; Sessoli, R. *J. Am. Chem. Soc.* **1991**, *113*, 5873. (b) McCusker, J. K.; Christmas, C. A.; Hagen, P. M.; Chadha, R. K.; Harvey, D. F.; Hendrickson, D. N. *J. Am. Chem. Soc.* **1991**, *113*, 6114. (c) Real, J. A.; De Munno, G.; Chiappetta, R.; Julve, M.; Lloret, F.; Journaux, Y.; Colin, J.-C.; Blondin, G. *Angew. Chem., Int. Ed. Engl.* **1994**, *33*, 1184. (d) Squire, R. C.; Aubin, S. M. J.; Folting, K.; Streib, W. E.; Hendrickson, D. N.; Christou, G. *Angew. Chem., Int. Ed. Engl.* **1995**, *34*, 887. (e) Taft, K. L.; Delfs, C. D.; Papaefthymiou, G. C.; Foner, S.; Gatteschi, D.; Lippard, S. J. *J. Am. Chem. Soc.* **1994**, *116*, 823. (f) Tsai, H.-L.; Wang, S.; Folting, K.; Streib, W. E.; Hendrickson, D. N.; Christou, G. *J. Am. Chem. Soc.* **1995**, *117*, 2503. (g) Halcrow, M. A.; Huffman, J. C.; Christou, G. *Angew. Chem., Int. Ed. Engl.* **1995**, *34*, 889. (h) Caneschi, A.; Cornia, A.; Fabretti, A. C.; Gatteschi, D. *Angew. Chem., Int. Ed. Engl.* **1995**, *34*, 2716. (i) Caneschi, A.; Cornia, A.; Lippard, S. J. *Angew. Chem., Int. Ed. Engl.* **1995**, *34*, 467. (j) Grillo, V. A.; Knapp, M. J.; Bollinger, J. C.; Hendrickson, D. N.; Christou, G. *Angew. Chem., Int. Ed. Engl.* **1996**, *35*, 1818.

(4) Mikuriya, M.; Kotera, T.; Adachi, F.; Bandow, S. *Chem. Lett.* **1993**, 945.

(5) (a) Gatteschi, D.; Pardi, L.; Barra, A.-L.; Müller, A. *Mol. Eng.* **1993**, *3*, 157. (b) Müller, A.; Rohlfing, R.; Barra, A.-L.; Gatteschi, D. *Adv. Mater.* **1993**, *5*, 915. (c) Khan, M. I.; Chen, Q.; Höpe, H.; Parkin, S.; O'Connor, C. J.; Zubieta, J. *Inorg. Chem.* **1993**, *32*, 2929. (d) Khan, M. I.; Chen, Q.; Goshorn, D. P.; Höpe, H.; Parkin, S.; Zubieta, J. *J. Am. Chem. Soc.* **1992**, *114*, 3341.

(6) Khan, M. I.; Lee, Y.-S.; O'Connor, C. J.; Zubieta, J. *J. Am. Chem. Soc.* **1994**, *116*, 5001.

(7) Plass, W. *Angew. Chem., Int. Ed. Engl.* **1996**, *35*, 627.

S0020-1669(96)01366-3 CCC: $14.00

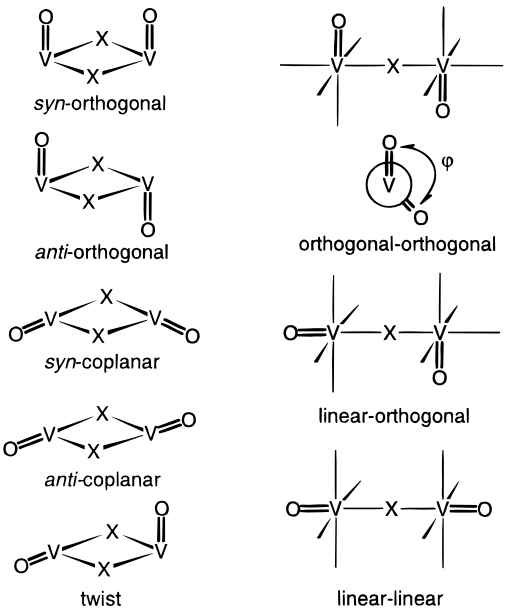

Figure 1. Possible configurations of the two terminal oxo groups for binuclear vanadium(IV) units with single-atom bridges which establish edge- (left) and vertex-shared bridging modes (right). The arrangements are classified according the orientation of the oxo groups with respect to the bridging plane in the case of edge-sharing units (orthogonal, coplanar, twist) or the connecting single-atom bridge for vertex-sharing units (linear, orthogonal) and the orientation of the two terminal oxo groups (*syn*, *anti*).

resulting generalized classification schemes for both edge- and vertex-sharing binuclear units with single-atom bridges are depicted in Figure 1. Considerations similar to those used to account for the magnetic behavior of edge-sharing binuclear oxovanadium(IV) complexes[7] can be applied to predict the magnetic interactions operative in the case of vertex-sharing binuclear units. Consequently, two of the possible configurations should lead to ferromagnetic interactions, namely the linear−linear and linear−orthogonal ones, whereas the orthogonal−orthogonal configuration depending on the dihedral angle φ can yield either antiferro- or ferromagnetic interactions, with the latter expected for φ near 90°. Within the scheme for vertex-shared binuclear units, the configurations also include the situations where one of the oxo groups is at the bridging position X, yielding either oxo-bridged units[6] or extended chains.[9] Consistent with the classification schemes given in Figure 1, the predominant magnetic exchange interactions observed for polynuclear oxovanadium(IV) clusters are of antiferromagnetic nature.[4−6]

Within the family of polynuclear transition-metal systems, tetranuclear clusters are of particular interest, as they are still simple enough for their magnetic interactions to be analyzed and, on the other hand, they already enable rather complex spin topologies.[2c,10] Although clusters with the tetrametalate core $\{M_4O_{16}\}$ are well-established for different transition-metal systems,[4,8,11] only one example solely containing oxovanadium(IV) centers is known, the cluster anion $[(VO)_4(H_2O)_2(SO_4)_2\{(OCH_2)_3CR\}_2]^{2-}$, which has been obtained under conditions of solvothermal synthesis.[12] However, the magnetochemistry of this cluster anion has not been examined. As a bridging ligand, the tris(hydroxymethyl)alkane used in the synthesis of this complex generally facilitates the formation of trigonal metal cores and, therefore, has been widely empolyed in the hydrothermal synthesis of polyalkoxometalate clusters.[8]

In the present study, a simple synthetic approach to neutral tetranuclear oxovanadium(IV) clusters at ambient conditions is described for potentially bridging and/or chelating amine alcohol ligand systems. Moreover, the structural, spectroscopic, and magnetic data of the synthesized oxovanadium(IV) cluster are presented. A detailed analysis of the magnetic data is performed and reveals interesting magnetic exchange interactions within the tetranuclear oxovanadium(IV) core.

Experimental Section

Preparation of *N*,*N*-Bis(2-hydroxyethyl)-*N*′-(2-pyrrolylmethylidene)ethylenediamine (H_2L). To a stirred solution of 2.70 g (18 mmol) of *N*,*N*-bis(2-hydroxyethyl)ethylenediamine in 50 mL of methanol was added 1.73 g (18 mmol) of 2-formylpyrrole dissolved in 10 mL of methanol. After the addition was complete, the reaction mixture was stirred at room temperature for 12 h, yielding a reddish brown solution. The solvent methanol was removed in vacuo, the resulting viscous oil dissolved in chloroform, and the solution dried with anhydrous sodium sulfate. The mixture was filtered and the chloroform removed under reduced pressure to afford a viscous oil; yield 3.53 g (87%).

^{1}H NMR (250 MHz, $CDCl_3$, δ in ppm): 2.73 (t, ^3J = 5.1 Hz, 4H), 2.78 (t, ^3J = 5.6 Hz, 2H), 3.52 (t, ^3J = 5.1 Hz, 2H), 3.57 (t, ^3J = 5.6 Hz, 4H), 6.10 (s, 2H), 6.17 (dd, 1H), 6.27 (m, 1H), 6.47 (dd, 1H), 6.86 (br s, 1H), 8.02 (s, 1H). ^{13}C NMR (63 MHz, $CDCl_3$, δ in ppm): 55.4, 57.3, 59.1, 59.4, 109.3, 115.1, 122.5, 129.3, 152.6. Selected IR data (neat between CsI plates, cm^{-1}): ν(O−H) 3350 br s, ν(C=N) 1638 vs.

Preparation of $[\{VO(L)\}_2\{VO(acac)\}_2(\mu_2\text{-}OMe)_2]\cdot$MeOH (1·MeOH). The reaction was carried out in an argon atmosphere using Schlenk line techniques with solvents purified prior to use. H_2L (0.68 g, 3.0 mmol) dissolved in 5 mL of methanol was added to a solution of 0.80 g (3.0 mmol) of $[VO(acac)_2]$ in 15 mL of methanol. The resulting red-brown solution was allowed to stand at room temperature. After 1−2 days, thin brown crystals of **1**· MeOH began to grow. After 5 days, **1**·MeOH was isolated by filtration and washed with methanol; yield 0.95 g (63%). The isolated solid material can be stored in air without any measurable decomposition.

Anal. Calcd for $C_{35}H_{58}N_6O_{15}V_4$: C, 41.76; H, 5.81; N, 8.35. Found: C, 41.89; H, 5.88; N, 8.43. Selected IR data (Nujol mull between CsI plates, cm^{-1}): ν(OH) 3420 br w, ν(NH) 3270 m, ν(V=O) 966 vs, ν(V=O) 954 vs. UV/vis (solid state, reflectance, $\tilde{\nu}_{max}$ in 10^3 cm^{-1}): 35.0, 22.6 (sh), 16.4 (sh), 11.4.

Physical Measurements. ^{1}H and ^{13}C{^{1}H} NMR spectra were recorded on a Bruker AC250 (^{1}H, 250.13 MHz; ^{13}C, 62.90 MHz) spectrometer. Chemical shifts δ are reported with reference to external tetramethylsilane. Solid samples for IR were measured as either KBr pellets or Nujol mulls between CsI plates, and liquid samples were measured neat between CsI plates on a Bruker IFS66 FT-IR spectrometer. UV/vis reflectance spectra of solid samples were measured on a Beckman Acta MIV spectrometer (cellulose as calibration standard). X-Band ESR spectra were recorded with a Bruker ECS106 spectrometer at a microwave frequencies of 9.48 GHz using 2,2-diphenyl-1-picrylhydrazyl as standard. Mangnetic susceptibility measurements from 4 to 280 K were performed by using a SQUID magnetometer. All data were collected in an applied field of 10 kOe. The diamagnetic corrections were estimated from Pascal's constants. The susceptibility

(8) Khan, M. I.; Zubieta, J. In *Progress in Inorganic Chemistry*; Karlin, K. D., Ed.; Wiley-Interscience: New York, 1995; Vol. 43, p 1.
(9) Mohan, M.; Bond, M. R.; Otieno, T.; Carrano, C. J. *Inorg. Chem.* **1995**, *34*, 1233.
(10) (a) McCusker, J. K.; Vincent, J. B.; Schmitt, E. A.; Mino, M. L.; Shin, K.; Coggin, D.; Hagen, P. M.; Huffman, J. C.; Christou, G.; Hendrickson, D. N. *J. Am. Chem. Soc.* **1991**, *113*, 3012. (b) Kirk, M. L.; Chan, M. K.; Armstrong, W. H.; Solomon, E. I. *J. Am. Chem. Soc.* **1992**, *114*, 10432. (c) Coronado, E.; Gómez-Garzía, C. J. *Comments Inorg. Chem.* **1995**, *17*, 255.
(11) (a) Cavaco, I.; Pessoa, J. C.; Duarte, M. T.; Matias, P. M.; Henriques, R. T. *Polyhedron* **1993**, *12*, 1231. (b) Crans, D. C.; Marshman, R. W.; Gottlieb, M. S.; Anderson, O. P.; Miller, M. M. *Inorg. Chem.* **1992**, *31*, 4939. (c) Chisholm, M. H.; Huffman, J. C.; Kirkpatrick, C. C.; Leonelli, J.; Folting, K. *J. Am. Chem. Soc.* **1981**, *103*, 6093.
(12) Chang, Y.; Chen, Q.; Khan, M. I.; Salta, J.; Zubieta, J. *J. Chem. Soc., Chem. Commun.* **1993**, 1872.

Table 1. Crystallographic Data for **1**·MeOH

formula	$C_{35}H_{58}N_6O_{15}V_4$
formula weight	1006.63
crystal size (mm^3)	0.05 × 0.25 × 0.30
crystal system	triclinic
space group	$P\bar{1}$
a (Å)	7.352(2)
b (Å)	12.584(4)
c (Å)	12.826(4)
α (deg)	107.61(2)
β (deg)	102.96(2)
γ (deg)	95.25(2)
V ($Å^3$)	1085.9(6)
Z	1
temp (K)	188
ρ_{calcd} (g/cm^3)	1.539
μ(Mo Kα) (mm^{-1})	0.907
$R1$[a]	0.071
$wR2$[b]	0.186

[a] $R1 = \Sigma||F_o| - |F_c||/\Sigma|F_o|$, calculated for all observed reflections. [b] $wR2 = [\Sigma w(F_o^2 - F_c^2)^2/\Sigma w(F_o^2)^2]^{1/2}$, with $w^{-1} = \sigma^2(F_o^2) + (0.07P)^2 + 2.25P$ and $P = {}^1/_3(\max(0,F_o^2) + 2F_c^2)$, calculated for all reflections used in refinement.

data used for the fit procedure were further corrected for temperature-independent paramagnetism (TIP) and the presence of paramagnetic impurity according to eq 1, where ρ is the fraction of paramagnetic

$$\chi_M (1 - \rho)\chi + \chi_{TIP} + \rho\chi_{mono} \quad (1)$$

impurity, χ_{mono} is the magnetic susceptibility from the monomer impurity, and χ_{TIP} is the temperature-independent paramagnetism. The parameters produced by the data fit are $\rho = 0.059$ and $\chi_{TIP} = 9.3 \times 10^{-4}$. Melting points (uncorrected) were determined with an electrothermal melting point apparatus. Elemental analyses were done using a LECO CHNS-932 analyzer.

Crystal Structure Determination. The crystallographic data of **1**·MeOH were collected on a Siemens R3m/V diffractometer, using graphite-monochromated Mo Kα ($\lambda = 0.710\ 73$ Å) radiation. The unit cell parameters were obtained by least-squares refinement of the angular settings from 23 reflections in the 2Θ range of 20−30°. Crystallographic data are given in Table 1, positional and equivalent isotropic thermal parameters in Table 2, and selected bond lengths and angles in Table 3.

Lorentz and polarization corrections as well as an absorption correction based on azimuthal Ψ scans were applied to the diffraction data (SHELXTL PLUS).[13] The structure was solved by direct methods (SHELXTL PLUS)[13] and subsequent full-matrix least-squares refinement of the function $\Sigma w(F_o^2 - F_c^2)^2$.[14] The pyrrole rings of the ligands L^{2-} were found to be disordered with respect to the orientation of the nitrogen atom N3, with refined site occupation factors of 0.7 for the molecule depicted in Figure 2. Consistent with the elemental analysis, one molecule of methanol from the crystallization solvent was found to be present in the unit cell. This molecule is disordered over two symmetry-related positions within the cavities established by the crystal lattice of **1**. As a consequence, the methanol molecule had to be refined as rigid group with isotropic thermal parameters and site occupation factors of 0.5 for the corresponding atoms O8 and C18. All other non-hydrogen atoms were refined with anisotropic displacement parameters. The hydrogen atoms were treated using the appropriate riding model and, for methyl groups, by additionally fitting their conformation to the difference Fourier map. The largest remaining peak in the final difference Fourier map was 1.2 e/$Å^3$, the magnitude of which probably reflects the poorly resolved disorder of the methanol molecule. The minimum negative peak was at 0.7 e/$Å^3$.

Results and Discussion

The amine alcohol ligand *N*,*N*-bis(2-hydroxyethyl)-*N*′-(2-pyrrolylmethylidene)ethylenediamine (H_2L), derived from the condensation reaction of *N*,*N*-bis(2-hydroxyethyl)ethylenediamine and 2-formylpyrrole, reacts with [VO(acac)$_2$] (Hacac = 2,4-pentanedione) to form the neutral tetranuclear oxovanadium(IV) complex [{VO(L)}$_2${VO(acac)}$_2$(μ_2-OMe)$_2$] (**1**). The reaction performed in methanol yields **1** as brown crystalline solid material, which is insoluble in common organic solvents like pentane, toluene, tetrahydrofuran, *N*,*N*-dimethylformamide, dimethyl sulfoxide, and alcohols. This is somewhat surprising

Table 2. Fractional Atomic Coordinates (×10^4) and Equivalent Isotropic Displacement Parameters U_{eq} (in 10^{-3} $Å^2$) for **1**·MeOH

	x/a	*y/b*	*z/c*	U_{eq}[a]
V1	−1489(2)	9142(1)	−1184(1)	29(1)
V2	355(2)	8200(1)	992(1)	33(1)
O1	−3616(6)	8770(3)	−1949(4)	38(1)
O2	−646(6)	7674(4)	1752(4)	41(1)
O3	1330(6)	9329(3)	−4(3)	29(1)
O4	−329(6)	10184(3)	−1813(4)	33(1)
O5	3058(6)	8423(3)	1897(4)	40(1)
O6	884(6)	6825(3)	−63(4)	38(1)
O7	−1867(6)	8158(3)	−233(4)	30(1)
N1	−113(7)	8017(4)	−2292(4)	30(1)
N2	−1573(9)	4910(5)	−4096(5)	51(2)
N3	−1663(11)	2036(6)	−4101(6)	60(2)
C1	−2827(12)	1059(6)	−4842(7)	55(2)
C2	−4038(11)	1337(6)	−5636(7)	50(2)
C3	−3588(10)	2500(6)	−5383(6)	52(2)
C4	−2123(12)	2918(6)	−4442(7)	50(2)
C5	−1065(12)	4065(6)	−3877(7)	52(2)
C6	−279(11)	6001(5)	−3547(6)	48(2)
C7	−1136(9)	6813(5)	−2725(6)	37(2)
C8	1914(8)	8084(5)	−1688(5)	31(1)
C9	2687(8)	9139(5)	−646(5)	32(1)
C10	−266(10)	8486(5)	−3237(5)	37(2)
C11	411(10)	9757(5)	−2764(6)	37(2)
C12	1997(11)	5116(5)	−716(6)	51(2)
C13	2087(10)	6219(5)	201(6)	40(2)
C14	3475(10)	6529(6)	1222(6)	46(2)
C15	3970(9)	7641(6)	1989(6)	38(2)
C16	5681(10)	7937(7)	2958(7)	55(2)
C17	−3461(10)	7275(5)	−555(7)	46(2)
O8	−4341(28)	4601(17)	−6016(17)	151(6)
C18	−3723(39)	5501(21)	−6349(24)	152(6)

[a] Equivalent isotropic U_{eq} defined as one-third of the trace of the orthogonalized $\mathbf{U}_{ij}$ tensor.

Table 3. Metal−Metal Distances and Selected Bond Lengths (Å) and Angles (deg) for **1**·MeOH

V1−O1	1.590(4)	V2−O2	1.597(5)
V1−O3	2.220(4)	V2−O3	2.343(4)
V1−O4	1.960(4)	V2−O4′	1.991(4)
V1−O3′	2.035(4)	V2−O5	2.010(5)
V1−O7	2.025(4)	V2−O6	1.980(4)
V1−N1	2.177(5)	V2−O7	1.981(4)
V1···V2	3.410(2)	V1···V2′	3.293(2)
V1···V1′	3.295(2)	V2···V2′	5.838(3)
O1−V1−O3	167.3(2)	O2−V2−O3	165.1(2)
O1−V1−O3′	107.1(2)	O2−V2−O4′	96.9(2)
O1−V1−O4	104.0(2)	O2−V2−O5	98.4(2)
O1−V1−O7	93.6(2)	O2−V2−O6	101.4(2)
O1−V1−N1	99.6(2)	O2−V2−O7	100.9(2)
O3−V1−O3′	78.6(2)	O3−V2−O4′	70.5(2)
O3−V1−O4	88.3(2)	O3−V2−O5	89.3(2)
O3−V1−O7	74.2(2)	O6−V2−O3	91.8(2)
O3−V1−N1	79.0(2)	O7−V2−O3	72.2(2)
O3′−V1−O4	78.1(2)	O4′−V2−O5	88.3(2)
O3′−V1−O7	98.0(2)	O4′−V2−O6	161.6(2)
O3′−V1−N1	148.2(2)	O4′−V2−O7	90.9(2)
O4−V1−O7	162.5(2)	O5−V2−O6	86.5(2)
O4−V1−N1	79.0(2)	O5−V2−O7	160.6(2)
O7−V1−N1	97.3(2)	O6−V2−O7	88.2(2)
V1−O3−V2	96.7(2)	V1−O4−V2′	112.9(2)
V1−O3−V1′	101.4(2)	V2−O7−V1	116.7(2)
V1′−O3−V2	97.3(2)		

(13) *SHELXTL PLUS*; Siemens Analytical X-Ray Instruments Inc., Madison, WI, 1989.
(14) Sheldrick, G. M. *SHELXL-93*; Universität Göttingen, Germany, 1993.

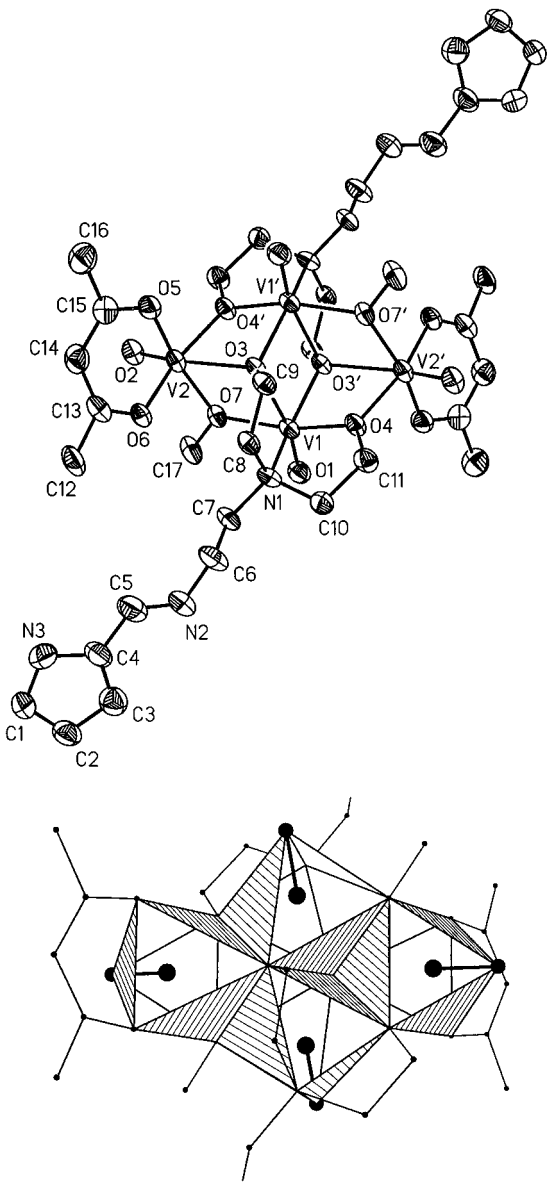

Figure 2. Molecular structure of **1** in crystals of **1**·MeOH. (Top) Thermal ellipsoids are drawn at the 50% probability level; atoms related by the crystallographic inversion center are denoted with a prime in the labeling scheme. (Bottom) Polyhedral representation of the $\{(VO)_4(\mu_3\text{-}OR)_2(\mu_2\text{-}OR)_4\}^{2+}$ core of **1**, with highlighted V═O groups.

since the imine functionality of the chelating and bridging ligand L^{2-} is not coordinated to any metal center of the cluster core, leaving a rather large dangling side chain. Under the given conditions, the complex **1** is formed for varying $[VO(acac)_2]$-to-ligand ratios; even with a 5-fold ligand excess, **1** was the only reaction product that could be identified.

The X-ray crystal structure analysis reveals that the complex **1** crystallizes in the centrosymmetric space group $P\bar{1}$ together with one molecule of methanol from the crystallization solvent. The presence of an additional methanol molecule is consitent with both the elemental analysis and the observed IR band at about 3400 cm^{-1} due to the O−H stretching vibration. The molecular structure of the neutral tetranuclear oxovanadium(IV) complex **1** is depicted in Figure 2. The tridentate ligand L^{2-} occupies three facial positions at the vanadium center V1, formally building a $\{VO(L)(OMe)\}^-$ fragment. Two of these fragments are arranged in an *anti*-coplanar configuration to form a central $[\{VO(L)(OMe)\}_2]^{2-}$ unit, with the ligand ethoxy oxygen donors O3 and O3′ at the bridging positions. This central unit provides two trigonal faces, each formed by three oxygen atoms for further aggregation (O3, O7, O4′ and O3′, O7′, O4). Condensation of two $\{VO(acac)\}^+$ fragments onto these trigonal faces finally builds the centrosymmetric tetranuclear core $\{(VO)_4(\mu_3\text{-}OR)_2(\mu_2\text{-}OR)_4\}^{2+}$ of **1**, with all four octahedrally coordinated oxovanadium(IV) centers linked in an edge-sharing fashion. This core structure corresponds to the well-established $\{M_4O_{16}\}$ condensation motif found for high-valent transition-metal systems,[4,8,11] which is characterized by two μ_3-bridging and four μ_2-bridging positions. In **1**, the alkoxy oxygen donors O3 and O4 occupy both μ_3- and μ_2-bridging positions, respectively. Although the given fragmentation pattern is solely of structurally descriptive origin, it seems likely that a growth process based on a similar but neutral and, therefore, protonated central fragment $[\{VO(L)(HOMe)\}_2]$ occurs, allowing further reaction with two additional molecules of $[VO(acac)_2]$. However, the binuclear aggregation intermediate in this growth process may also be a $[\{VO(L)\}_2]$ fragment, which is stabilized by coordination of the dangling Schiff base instead of an additional methanol molecule.

Overall, the $\{(VO)_4(\mu_3\text{-}OR)_2(\mu_2\text{-}OR)_4\}^{2+}$ core of **1** exhibits five-edge shared binuclear arrangements: one with *anti*-coplanar (V1···V1′ = 3.295(2) Å), two with *syn*-coplanar (V1···V2 and V1′···V2′ = 3.410(2) Å), and two with twist configuration (V1···V2′ and V1′···V2 = 3.293(2) Å). This orientation pattern of the oxo groups is directed by the *trans* effect generally observed for this strong terminal ligand, as they are all four arranged *trans* to the μ_3-bridging alkoxy oxygen donors O3 and O3′. This is reflected in the observed related bond lengths summarized in Table 3. The rather short V═O bond lengths of 1.590(4) and 1.597(5) Å are consistent with the observed frequencies of the two IR bands related to the V═O stretching vibrations at 954 and 966 cm^{-1}. For the μ_2-bridging alkoxy oxygen donors O4 and O7, a trigonal planar environment is observed (sum of the angles around O4, 360°, and O7, 358°), whereas the environment of the μ_3-bridging donor O3 is slightly distorted from the expected pyramidal coordination geometry.

The X-band ESR powder spectrum of **1**·MeOH recorded at room temperature shows a broad unstructured band at $g = 1.97$ and a second weak resonance at half-field, indicating that the spectrum is the result of an exchange-coupled spin system.[15] The temperature dependence of the resonance signal indicates a singlet ground state for **1**, and at very low temperatures, only the resonance signal of a residual monomeric oxovanadium(IV) impurity can be detected.

The magnetic susceptibility χ of a polycrystalline sample of **1**·MeOH was measured in a temperature range from 4 to 280 K. The temperature dependence of the molar magnetic susceptibility χ_M and the product $\chi_M T$ is shown in Figure 3. χ_M goes through a maximum at about 135 K and is increasing again below 25 K due to the presence of paramagnetic impurities. The observed low-temperature value of $\chi_M T$ is in accord with an $S = 0$ ground state of **1**, as suggested by the ESR spectra. Moreover, the temperature dependence of $\chi_M T$ clearly indicates that antiferromagnetic exchange interactions must be operative within the tetranuclear core of **1**.

On the basis of the magnetostructural relationship given in Figure 1, both antiferro- and ferromagnetic interactions can be expected to be operative within the $\{(VO)_4(\mu_3\text{-}OR)_2(\mu_2\text{-}OR)_4\}^{2+}$ core of **1**. The spin topology and the notation of the mangetic exchange interaction parameters are depicted in Figure 4. Given the close similarities between the structural parameters of the *anti*-coplanar (V1···V1′) and twist arrangements (V1···V2′ and V1′···V2) of **1** and those observed for the binuclear complexes

(15) Bencini, A.; Gatteschi, D. *Electron Paramagnetic Resonance of Exchange Coupled Systems*; Spinger: Berlin, 1990.

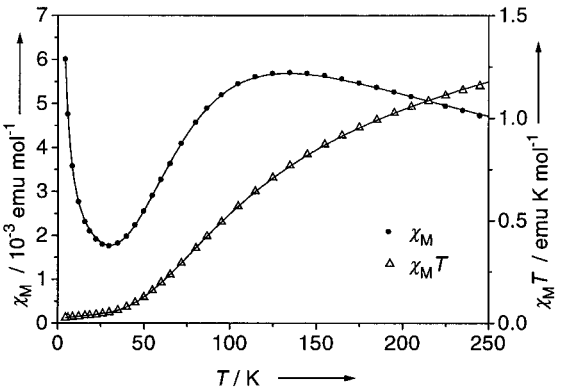

Figure 3. Temperature dependence of the molar magnetic susceptibility χ_M (●) and the product of the molar magnetic susceptibility with temperature $\chi_M T$ (△) for **1**·MeOH. The solid lines represent the calculated values (see text).

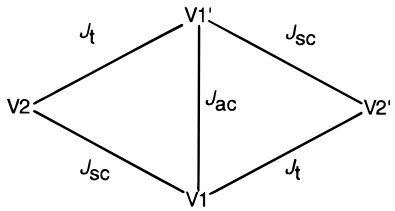

Figure 4. Spin topology of the $\{(VO)_4(\mu_3\text{-}OR)_2(\mu_2\text{-}OR)_4\}^{2+}$ core of **1** with the magnetic exchange coupling constants denoted as follows: J_{ac}, *anti*-coplanar; J_{sc} *syn*-coplanar; and J_t, twist configurations.

[{VO(Hsabhea)}$_2$] (*anti*-coplanar, V···V = 3.307 Å) and [{VO(Hsabhea)}{VO(acac)(HOMe)}(μ_2-OMe)] (twist, V···V = 3.225 Å),[7] respectively, weak ferromagnetic interactions on the order of 5−10 cm^{-1} can be expected for the corresponding magnetic exchange parameters J_{ac} and J_t. For binuclear complexes exhibiting *syn*-coplanar configurations, only one example has been reported, $NH_4[V_2O_2(OH_2)_2(\mu\text{-}OH)(\mu\text{-}OH_2)(C_4O_4)_2]\cdot H_2O$, indicating strong antiferromagnetic exchange interactions between the two vanadium(IV) centers (V···V = 3.33 Å, J = −334 cm^{-1}).[16] Therefore, despite the long V···V distance of 3.41 Å, a rather strong antiferromagnetic coupling constant, J_{sc}, can be expected on the basis of the possible superexchange mechanism through the corresponding bridging methoxy oxygen donors (O7 and O7′). As a consequence of the given spin topology (see Figure 4), the expected antiferro- (J_{ac} and J_t) and ferromagnetic exchange interactions (J_{sc}) cannot be simultaneously satisfied.

Such a situation with competing magnetic exchange interactions within a tetranuclear core arrangement can basically yield different spin ground states depending on the relative ratio of the exchange interaction parameters involved, here J_{sc}, J_{ac}, and J_t. Given a situation as outlined for **1**, with $-J_{sc} \gg J_{ac} \approx J_t$, both pairs with *syn*-coplanar configuration (V1···V2 and V1a···V2a) should be predominantly coupled to form two virtually independent $S = 0$ ground states. To prove this simplified binuclear model, a quantitative analysis of the susceptibility data corrected for diamagnetism and further corrected for temperature-independent paramagnetism (TIP) and the presence of paramagnetic impurity (cf. Experimental Section and eq 1) has been performed using the Heisenberg−Dirac−van Vleck Hamiltonian given in eq 2.

$$\hat{\mathbf{H}} = -J(\hat{\mathbf{S}}_1\cdot\hat{\mathbf{S}}_2 + \hat{\mathbf{S}}_{1'}\cdot\hat{\mathbf{S}}_{2'}) \qquad (2)$$

The magnetic parameters derived for the simplified isotropic spin Hamiltonian according to eq 2 are $g = 1.88$ and $J = -152$ cm^{-1}. Although only one exchange interaction constant is used

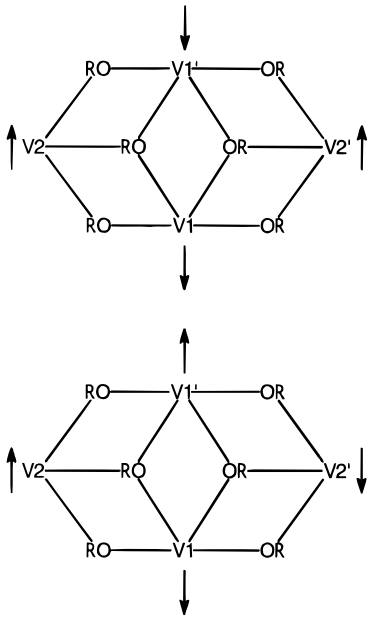

Figure 5. Sketch of the possible spin alignments for the $\{(VO)_4(\mu_3\text{-}OR)_2(\mu_2OR)_4\}^{2+}$ core of **1**.

in the analytical expression, a reasonably good fit to the experimental data can be achieved, thereby supporting the initial qualitative picture.

For the detailed analysis of the magnetic data, isotropic exchange interactions according to Figure 4 have been assumed, which yield the Heisenberg−Dirac−van Vleck Hamiltonian given in eq 3.

$$\hat{\mathbf{H}} = -J_{ac}\hat{\mathbf{S}}_1\cdot\hat{\mathbf{S}}_{1'} - J_t(\hat{\mathbf{S}}_1\cdot\hat{\mathbf{S}}_{2'} + \hat{\mathbf{S}}_{1'}\cdot\hat{\mathbf{S}}_2) - J_{sc}(\hat{\mathbf{S}}_1\cdot\hat{\mathbf{S}}_2 + \hat{\mathbf{S}}_{1'}\cdot\hat{\mathbf{S}}_{2'}) \qquad (3)$$

The general susceptibility expression (eq 4), as derived[17] from the general van Vleck equation, was used for fitting experimental

$$\chi = \frac{2Ng^2\beta^2}{kT} \times \frac{5e^{-E_Q/kT} + e^{-E_{T1}/kT} + e^{-E_{T2}/kT} + e^{-E_{T3}/kT}}{5e^{-E_Q/kT} + 3e^{-E_{T1}/kT} + 3e^{-E_{T2}/kT} + 3e^{-E_{T3}/kT} + e^{-E_{S1}/kT} + e^{-E_{S2}/kT}} \qquad (4)$$

χ data by using a nonlinear regression program, where $E_Q = -1/2(J_{ac} + 2J_t + 2J_{sc})$, $E_{T1} = -1/2(J_{ac} - 2J_t - 2J_{sc})$, $E_{T2} = 1/2[J_{ac} + 2(J_{ac}^2 + (J_t - J_{sc})^2)^{1/2}]$, $E_{T3} = 1/2[J_{ac} - 2(J_{ac}^2 + (J_t - J_{sc})^2)^{1/2}]$, $E_{S1} = 1/2[J_{ac} + 2J_t + 2J_{sc} + 2((J_{ac} - J_t - J_{sc})^2 + 3(J_t - J_{sc})^2)^{1/2}]$, and $E_{S2} = 1/2[J_{ac} + 2J_t + 2J_{sc} - 2((J_{ac} - J_t - J_{sc})^2 + 3(J_t - J_{sc})^2)^{1/2}]$.

As shown in Figure 3, the theoretical model based on the Hamiltonian given in eq 3 is in good agreement with the experimental susceptibility data if J_{sc} is taken from the simplified binuclear model (−152 cm^{-1}) and the additional exchange parameters $J_{ac} = +3$ cm^{-1} and $J_t = +11$ cm^{-1} are chosen according the data available for binuclear model complexes with *anti*-coplanar and twist configuration.[7]

A full refinement of the parameter set yields $g = 1.86$, $J_{sc} = -153$ cm^{-1}, $J_{ac} = +1$ cm^{-1}, and $J_t = +1$ cm^{-1}, with ρ and

(16) (a) Kahn, M. I.; Chang, Y.-D.; Chen, Q.; Salta, J.; Lee, Y.-S.; O'Connor, C. J.; Zubieta, J. *Inorg. Chem.* **1994**, *33*, 6340. (b) Müller, A.; Rohlfing, R.; Krickemeyer, E.; Bögge, H. *Angew. Chem., Int. Ed. Engl.* **1993**, *32*, 909.

(17) (a) Sinn, E. *Coord. Chem. Rev.* **1970**, *5*, 313. (b) Hall, J. W.; Estes, W. E.; Estes, E. D.; Scaringe, R. P.; Hatfield, W. E. *Inorg. Chem.* **1977**, *16*, 1572.

χ_{TIP} at the values given in the Experimental Section. Although the values obtained for J_{ac} and J_t are within the expected range for weak ferromagnetic exchange interactions, they are, in contrast to J_{sc}, not well-defined, with error margins of about 50 cm^{-1}. This leaves J_{ac} and J_t virtually undefined, ranging from weak ferromagnetic (about $+5$ cm^{-1}) to moderate antiferromagnetic exchange interactions (about -30 cm^{-1}). Within this range, the susceptibility data can be reproduced satisfactorily.

This effect can be rationalized by the competition of the two possible spin alignments depicted in Figure 5, since for both spin patterns one of the two preferred ferromagnetic interactions (J_{ac} or J_t) cannot be satisfied. This is reflected in the indeterminante nature of the two exchange interaction parameters J_{ac} and J_t and is often related to spin frustration phenomena, although these essentially refer to competing interactions which lead to degenerate ground states.[2c] Similar effects are also found for tetranuclear clusters of other transition metals with the metal centers disposed in a so-called "butterfly" arrangement.[10,18] The corresponding spin topology is characterized by two triangular metal arrangements fused over one shared edge. For such an arrangement, the observation of "spin frustration" phenomena is directly related to the occurrence of competition effects within the exchange coupling pattern of the cluster core.

(18) (a) Casañ-Pastor, N.; Bas-Serra, J.; Coronado, E.; Pourroy, G.; Baker, L. C. W. *J. Am. Chem. Soc.* **1992**, *114*, 10380. (b) Gómez-Garzía, C. J.; Coronado, E.; Borrás-Almenar, J. J. *Inorg. Chem.* **1992**, *31*, 1667. (c) Gómez-Garzía, C. J.; Coronado, E.; Gómez-Romero, P.; Casañ-Pastor, N. *Inorg. Chem.* **1993**, *32*, 3378.

Conclusions

A synthetic approach to tetranuclear oxovanadium(IV) clusters with amine alcohol ligands at ambient conditions is presented. The presence of an imine functionality in the ligand system should facilitate the chemical modification of the resulting complex system with respect to its chemical and physical properties. The synthesized complex **1** is the first example of a neutral tetranuclear oxovanadium(IV) cluster with edge-sharing octahedral units. The analysis of the magnetic data reveals competing magnetic exchange interactions, which lead to "spin frustration" phenomena characteristic for cluster cores with a "butterfly" arrangement, as it is found for the $\{(VO)_4(\mu_3\text{-}OR)_2(\mu_2\text{-}OR)_4\}^{2+}$ core of **1**. Moreover, the analysis of the magnetic data allows for the determination of the magnetic exchange interaction constant of the binuclear unit with *syn*-coplanar configuration. The derived value of $J_{sc} = -153$ cm^{-1} is in agreement with the magnetostructural correlation outlined in Figure 1 and the proposed superexchange mechanism.

Acknowledgment. This work was supported by the Deutsche Forschungsgemeinschaft, the Fonds der Chemischen Industrie, and the Herbert Quandt-Stiftung der VARTA AG. I am thankful to Dr. R. Sessoli, Florence, for the measurement of the magnetic suceptibility data and to Prof. Dr. A. Müller for his continuous support.

Supporting Information Available: An X-ray crystallographic file, in CIF format, is available. Access information is given on any current masthead page.

IC9613669